QUANTITATIVE FINANCE
RESEARCH CENTRE

UNIVERSITY OF
TECHNOLOGY SYDNEY

QUANTITATIVE FINANCE
RESEARCH CENTRE

UTS

THINK.CHANGE.DO

Quantitative Finance Research Centre

Research Paper 234 **August 2008**

On the Numerical Stability of Simulation Methods for SDES

Eckhard Platen and Lei Shi

ISSN 1441-8010

On the Numerical Stability of Simulation Methods for SDEs

Eckhard Platen[1] and **Lei Shi**[2]

August 29, 2008

Abstract. When simulating discrete time approximations of solutions of stochastic differential equations (SDEs), numerical stability is clearly more important than numerical efficiency or some higher order of convergence. Discrete time approximations of solutions of SDEs are widely used in simulations in finance and other areas of application. The stability criterion presented is designed to handle both scenario simulation and Monte Carlo simulation, that is, strong and weak simulation methods. The symmetric predictor-corrector Euler method is shown to have the potential to overcome some of the numerical instabilities that may be experienced when using the explicit Euler method. This is of particular importance in finance, where martingale dynamics arise for solutions of SDEs and diffusion coefficients are often of multiplicative type. Stability regions for a range of schemes are visualized and discussed. For Monte Carlo simulation it turns out that schemes, which have implicitness in both the drift and the diffusion terms, exhibit the largest stability regions. It will be shown that refining the time step size in a Monte Carlo simulation can lead to numerical instabilities.

1991 *Mathematics Subject Classification:* primary 65C20; secondary 60H10.
Key words and phrases: Stochastic differential equations, scenario simulation, Monte Carlo simulation, numerical stability, predictor-corrector methods, implicit methods.

[1]University of Technology, Sydney, School of Finance & Economics and Department of Mathematical Sciences, PO Box 123, Broadway, NSW, 2007, Australia
[2]University of Technology, Sydney, Australia, School of Finance & Economics

1 Introduction

Simulation methods for the approximate solution of stochastic differential equations (SDEs) have become widely used tools in finance and also in many areas of applications. Monographs describing these methods include, for instance, Kloeden & Platen (1999), Milstein (1995), Kloeden, Platen & Schurz (2003), Jäckel (2002) and Glasserman (2004). Not everyone who uses these tools in scenario simulation or Monte Carlo simulation is aware of potential problems that can make such a simulation worthless. The main problem concerns the uncontrolled propagation of errors during the simulation of an approximate path. If the impact of naturally arising errors is inappropriately propagated over time, then the approximate path simulated may diverge substantially from the exact solution in a scenario simulation. Similarly, the expectation of a functional estimated by a Monte Carlo simulation may be significantly different from that of the expected functional of the underlying SDE due to numerical instabilities. It is well known that for larger time step sizes explicit methods, in particular, the widely used Euler method, work unreliably and sometimes generate large errors, see for instance Milstein, Platen & Schurz (1998). This phenomenon can be avoided or at least controlled when using appropriate discrete time schemes, including predictor corrector methods or implicit schemes.

Implicit methods can successfully be used to control the propagation of errors. For this type of methods we refer to, for instance, papers by Talay (1982), Klauder & Petersen (1985), Milstein (1988), Hernandez & Spigler (1992, 1993), Saito & Mitsui (1993a, 1993b), Kloeden & Platen (1992, 1999), Milstein, Platen & Schurz (1998), Higham (2000) and Alcock & Burrage (2006). For scenario simulation, that is the strong approximate solution of SDEs, it is not straightforward to introduce implicitness into the discrete time approximation of the diffusion terms. Naive attempts lead typically to terms involving the inverse of Gaussian random variables, which can create division by zero and, thus, make numerically no sense. For SDEs with zero drift, as often encountered in finance when modelling martingales, there is no possibility for making the drift term in a scheme implicit. Balanced implicit methods may help to stabilize the numerical approximation in such a situation. This type of methods have been proposed in Milstein, Platen & Schurz (1998) and became later extended, for instance, in Alcock & Burrage (2006). Here one introduces some implicitness into the approximation of the diffusion term by adding an appropriate higher order term to a standard scheme. This additional term can significantly improve the numerical stability of the scheme. However, the disadvantage of implicit methods is that, in general, an algebraic equation has to be solved at each time step, which can cost significant computational time.

It is well known that for the case of deterministic ordinary differential equations predictor-corrector methods achieve improved numerical stability when compared with other explicit methods, see Hairer, Nørsett & Wanner (1987). This kind of method does not require solving an algebraic equation in each time step. In Platen (1995) and Kloeden & Platen (1999), predictor-corrector methods have been described for weak discrete time approximations. These methods can be used in Monte Carlo simulation. For the strong discrete time approximation of solutions of SDEs a family of predictor-corrector Euler methods has been developed in Bruti-Liberati & Platen (2008), which can be conveniently used to improve the numerical stability of a scenario simulation. This raises the question, which members of this family have good numerical stability properties for certain types of SDEs? Furthermore, the numerical stability of any other scheme that could be used would need to be systematically compared and analyzed.

The aim of the current paper is to provide a unified approach to the study of the numerical stability of schemes for the discrete time approximation of SDEs. We will introduce and apply a numerical stability criterion which allows one to visualize the corresponding stability regions of given schemes. The numerical stability of a method will be examined in relation to the concept of asymptotic stability and stronger forms of stability by using a family of linear test equations with multiplicative noise. Several numerical stability concepts known from the literature can be conveniently related to the proposed criterion. The visualization of the resulting stability regions for different schemes is an important aspect of our study. One obtains through the study of the shape of the stability region important insight into the stability properties of the respective scheme. This allows one to make informed decisions about the selection of an appropriate scheme for a given simulation task. An important effect will be pointed out where for some schemes the refinement in the time discretization can lead to numerical instabilities, which can cause serious problems in simulation.

This paper is organized as follows: Section 2 describes a family of strong predictor-corrector Euler schemes. Section 3 introduces a general concept of numerical stability. In Section 4, stability regions for various predictor-corrector methods are discussed. Section 5 studies the stability regions of particular implicit schemes. Finally, Section 6 discusses the numerical stability of a range of methods that are designed for Monte Carlo simulation.

2 Strong Predictor-Corrector Euler Schemes

Within this section we describe some strong discrete time approximations of solutions of SDEs. First, let us consider the solution $X = \{X_t, t \geq 0\}$ of the SDE

$$X_t = X_0 + \int_0^t a(X_s)\,ds + \int_0^t b(X_s)\,dW_s \tag{2.1}$$

for $t \geq 0$. Here $X_0 \in \Re$ denotes the deterministic initial value. The function $a : \Re \to \Re$ is the drift function. The function $b : \Re \to \Re$ denotes the diffusion coefficient function with respect to the Wiener process $W = \{W_t, t \geq 0\}$ that drives the dynamics of the solution X_t of the SDE (2.1). Additionally, we will use in our analysis the adjusted drift function $\bar{a}_\eta$ for $\eta \in [0,1]$ with

$$\bar{a}_\eta(x) = a(x) - \eta b(x) b^{'}(x), \tag{2.2}$$

for $x \in \Re$, where $b^{'}(x)$ denotes the first derivative of $b(.)$.

To ensure existence and uniqueness of the solution of the SDE (2.1) on a finite interval $[0,T]$, $T < \infty$, and also convergence of most schemes, we assume the Lipschitz condition

$$|a(x) - a(y)| + |\bar{a}_\eta(x) - \bar{a}_\eta(y)| + |b(x) - b(y)| \leq K\, |x - y|, \tag{2.3}$$

and the linear growth condition

$$|a(x)| + |\bar{a}_\eta(x)| + |b(x)| \leq K\,(1 + |x|). \tag{2.4}$$

Note that most of the results we present can be generalized to time inhomogeneous SDEs and also to multi-dimensional SDEs driven by several Wiener processes.

The Euler scheme is the simplest and most popular scheme for the discrete time approximation of SDEs, see Kloeden & Platen (1999). It simply keeps the drift and diffusion coefficients constant over the discretization interval. The Euler scheme has the form

$$Y_{n+1} = Y_n + a(Y_n)\Delta_n + b(Y_n)\Delta W_n. \tag{2.5}$$

It is an explicit scheme and is known to exhibit numerical instabilities for particular SDEs and large time step sizes. For instance, in Milstein, Platen & Schurz (1998) it has been demonstrated that for a martingale, modelled by geometric Brownian motion, the simulation of the solution of the corresponding SDE can be rather erratic if the time step size is not small enough.

For simplicity, in the schemes we consider we will mention only the one-dimensional time homogeneous case. Let us consider a time discretization $0 = t_0 < t_1 < \ldots$ with equal time step size $\Delta = t_{n+1} - t_n$, $n \in \{0, 1, \ldots\}$. The corresponding increments of the Wiener process are denoted by $\Delta W_n = W_{t_{n+1}} - W_{t_n}$, $n \in \{0, 1, \ldots\}$. We denote by $Y_n = Y_{t_n}$ the value of a discrete time approximation at time t_n, and by $n_t = \max\{n \in \{0, 1, \ldots\} : t_n \leq t\}$ the largest integer n for which t_n does not exceed $t \geq 0$. The following strong predictor-corrector schemes generalize the Euler scheme and can provide some improved numerical stability, while avoiding to solve an algebraic equation in each time step, as is required by implicit methods. At the nth time step, first the *predictor* is constructed by using an explicit Euler scheme which predicts a value $\bar{Y}_{n+1}$. Afterwards, the *corrector* is applied, which is in its structure similar to an implicit Euler scheme and corrects the predicted value. We emphasize that not only the predictor step is explicit, but also the corrector step is explicit since it only uses the predicted value. We will see later that with such a two-step predictor-corrector procedure one can introduce some stabilizing effect in the simulation and can avoid errors to be propagated. The *family of strong predictor-corrector Euler schemes* we consider is given by the *corrector*

$$\begin{aligned} Y_{n+1} &= Y_n + \left\{ \theta\, \bar{a}_\eta(\bar{Y}_{n+1}) + (1-\theta)\bar{a}_\eta(Y_n) \right\} \Delta \\ &\quad + \left\{ \eta\, b(\bar{Y}_{n+1}) + (1-\eta)\, b(Y_n) \right\} \Delta W_n, \end{aligned} \tag{2.6}$$

and by the *predictor*

$$\bar{Y}_{n+1} = Y_n + a(Y_n)\,\Delta + b(Y_n)\,\Delta W_n. \tag{2.7}$$

Note that we need to use in (2.6) the adjusted drift function $\bar{a}_\eta = a - \eta\, b\, b'$. The parameters $\theta, \eta \in [0,1]$ are called the degree of implicitness in the drift and the diffusion coefficient, respectively. For the case $\eta = \theta = 0$ one recovers the Euler scheme in (2.5). A major advantage of the above family of schemes is that they have flexible degree of implicitness parameters η and θ. For each possible combination of these two parameters the scheme is of strong order 0.5 in the sense of Kloeden & Platen (1999), see Bruti-Liberati & Platen (2008). This allows one to compare for a given problem simulated paths for different degrees of implicitness. If these paths differ significantly from each other, then some numerical stability problem is likely to be present and one needs to make an effort in providing extra numerical stability. The above strong predictor-corrector schemes offer potentially the required numerical stability. However, other schemes, in particular, implicit schemes may have to be employed to secure sufficient numerical stability for a given simulation task. Such implicit schemes will be introduced later when we study their numerical stability properties. It will then turn out that by reducing the time step size some schemes can lose their numerical stability.

3 Numerical Stability

One of the common tasks in numerical analysis is to choose algorithms which are *numerically stable* for the task at hand. The precise definition of numerical stability depends on the context, but it is typically related to the long term accuracy of the algorithm when applied to the given dynamics. In the context of solving SDEs via simulation, one can use different discrete time approximations with different orders of convergence to simulate the paths of an approximating stochastic process. However, numerical errors such as roundoff and truncation errors are unavoidable during simulations on a digital computer. Therefore, it is important to choose a numerical scheme which dampens approximation errors or at least does not magnify these. In comparison with the widely discussed concepts of strong or weak order of convergence, the question on numerical stability should be answered first when deciding which numerical scheme to use. Computational efficiency is a secondary issue.

Various concepts of numerical stability have been introduced in the literature for numerical schemes approximating solutions of SDEs. These concepts typically make use of specifically designed test equations, which have explicit solutions available, see, for instance, Milstein (1995), Kloeden & Platen (1999), Hernandez & Spigler (1992, 1993), Saito & Mitsui (1993a, 1993b, 1996), Hofmann & Platen (1994, 1996) and Higham (2000). Under such concept one can systematically analyze the stability properties of a numerical scheme for the given family of test equations. Moreover, these test equations are often designed to have solutions which are themselves asymptotically stable according to a given stability criterion. This typically means that the solution approaches zero over time for the admissible parameter range. Along similar lines, the stability of a numerical scheme refers to the property that the numerical approximation of the solution tends to zero as time tends to infinity.

There have been various efforts made in the literature trying to visualize numerical stability for a given scheme by using some test equations. Stability regions have been identified for the parameter sets where the propagation of errors is under control in a well-defined sense. In some cases authors use solutions of complex valued linear SDEs with additive noise as test dynamics, see Milstein (1995), Kloeden & Platen (1999) and Hernandez & Spigler (1992, 1993) and Higham (2000). However, in financial applications, these test equations are potentially not realistic enough to capture typically arising numerical instabilities. For example, when simulating the dynamics of asset prices, benchmarked against a certain numeraire, the resulting SDE has no drift and its diffusion coefficient is often level dependent in a multiplicative manner. To study the stability of corresponding numerical schemes for dynamics with level dependent diffusion coefficients, test SDEs with multiplicative noise have been suggested in real valued and complex valued form, see Saito & Mitsui (1993a, 1993b, 1996), Hofmann & Platen (1994, 1996) and Higham (2000). Recently, Bruti-Liberati & Platen (2008) analyzed the stability regions of a family of strong predictor-corrector Euler schemes under a criterion which analyzes a rather weak form of numerical stability, the asymptotic stability.

In the spirit of Bruti-Liberati & Platen (2008), the current paper introduces a general stability criterion. The criterion unifies to some extent those criteria that exploit asymptotic stability, mean square stability and stability of absolute moments. We then calculate corresponding stability regions to visualize the stability properties for a range of numerical schemes. The interpretation of these plots will turn out to be rather informative and intuitive. The methodology can be employed for the study of numerical stability properties of both strong and weak schemes.

Similar to Hofmann & Platen (1994) and Bruti-Liberati & Platen (2008) we use a *linear test SDE* with *multiplicative noise*. Its explicit solution is of the form

$$X_t = X_0 \exp\left\{(1-\alpha)\,\lambda\,t + \sqrt{\alpha\,|\lambda|}\,W_t\right\} \tag{3.1}$$

for $t \geq 0$, $\lambda < 0$ and $\alpha \geq 0$. Here we call α the degree of stochasticity and λ the growth parameter. For $p > 0$ and $\lambda < 0$ it follows from (3.1), by application of Itô's formula and taking expectation, that

$$\lim_{t\to\infty} E(|X_t|^p) = 0 \tag{3.2}$$

if and only if $\alpha < \frac{1}{1+\frac{p}{2}}$. This means, in the case when $\lambda < 0$ and $\alpha \in [0, \frac{1}{1+p/2})$, roundoff errors occurring will not be relevant in the long-run. Similarly, for $\lambda < 0$ by the law of iterated logarithm and the law of large numbers, one has

$$P\left(\lim_{t\to\infty} X_t = 0\right) = 1 \tag{3.3}$$

if and only if $\alpha \in [0, 1)$, see for instance Protter (2004).

There is only limited potential for identifying numerically stable schemes for unstable test dynamics. Therefore, we will consider the family of test dynamics given by (3.1) only for negative growth parameter $\lambda < 0$ and degree of stochasticity $\alpha \in [0, 1)$. The process $X = \{X_t, t \geq 0\}$ satisfies the linear Itô SDE with multiplicative noise

$$dX_t = \left(1 - \frac{3}{2}\,\alpha\right)\lambda\,X_t\,dt + \sqrt{\alpha\,|\lambda|}\,X_t\,dW_t \tag{3.4}$$

for $t \geq 0$, where $X_0 > 0$, $\lambda < 0$, $\alpha \in [0, 1)$. The corresponding Stratonovich SDE has the form

$$dX_t = (1-\alpha)\,\lambda\,X_t\,dt + \sqrt{\alpha\,|\lambda|}\,X_t \circ dW_t, \tag{3.5}$$

where "$\circ$" denotes the Stratonovich stochastic integral, see Kloeden & Platen (1999).

For the two equivalent real valued SDEs (3.4) and (3.5), the parameter $\alpha \in [0, 1)$ describes the degree of stochasticity of the test dynamics. When $\alpha = 0$, the SDEs (3.4) and (3.5) become deterministic.

In the case $\alpha = \frac{2}{3}$, the Itô SDE (3.4) has no drift, and X is a martingale. This case models a typical Black-Scholes asset price dynamics when the price is expressed in units of a numeraire under the corresponding pricing measure. When the numeraire is the savings account, then the pricing measure is, under appropriate assumptions, the risk neutral probability measure. Platen & Heath (2006) show that the pricing measure is simply the real-world probability when the numeraire is taken to be the, so-called, *growth optimal portfolio*. In the case $\alpha = 1$, the Stratonovich SDE (3.5) has no drift. This is also the largest α for which the dynamics in (3.1) is potentially a useful test dynamics when considering negative $\lambda < 0$.

Now, let us introduce the following stability criterion:

Definition 3.1 *For $p > 0$ a process $Y = \{Y_t, t > 0\}$ is called* p-stable *if*

$$\lim_{t\to\infty} E(|Y_t|^p) = 0. \tag{3.6}$$

Consequently, a process is p-stable if in the long run its pth moment vanishes. By the Lyapunov inequality it follows that if a process is p_1-stable, for $p_1 > p_2 > 0$, then it is also p_2 stable. From (3.2) it follows that for all $\alpha \in [0, \frac{1}{1+p/2})$ and $\lambda < 0$ the solution process X, given in (3.1), is *p-stable.*

Numerically, one would like to see that a discrete time approximation Y and the original continuous process X have similar stability properties according to Definition 3.1. Ideally, for given $p > 0$ both X and Y should generate p-stable paths. Any impact from roundoff errors should decline over time when $\lambda < 0$ and $\alpha \in [0, \frac{1}{1+p/2})$. In our subsequent analysis we will see that this is generally not the case. Y and X typically have different stability properties for different combinations of values of $\lambda\Delta$, α and p. To explore these differences, we introduce for a given discrete time approximation the notion of a stability region which will permit the convenient visualization of its numerical stability properties.

Definition 3.2 *The* stability region Γ *is determined by those triplets* $(\lambda\Delta, \alpha, p)$ $\in (-\infty, 0) \times [0, 1) \times (0, \infty)$ *for which the discrete time approximation Y with time step size Δ, when applied to the test equation* (3.5)*, is p-stable.*

There exists a wide range of numerical stability concepts in the literature. For scenario simulation, Bruti-Liberati & Platen (2008) argued that the, so called, asymptotic stability is required, since one needs only to control the propagation of errors in a pathwise sense. If the impact of errors diminishes for a path in the long run, then the numerical scheme should appear to be suitable for long-term scenario simulation.

In Monte Carlo simulations, where expectations of functionals are approximated, also some moments of a discrete time approximation need to exhibit certain stability. Otherwise, errors in the expectations of functionals may be uncontrollably propagated. To correctly approximate the pth moment of a stochastic process X, given that its pth moment exists, the numerical approximation Y needs to be p-stable. This means that the pth moment of the approximation Y should asymptotically vanish for $t \to \infty$ if the one of the true solution X vanishes.

Note that the p-stability criterion (3.6) can be related to other concepts of numerical stability previously introduced in the literature, such as the popular concept of mean-square stability, see Saito & Mitsui (1996), Higham (2000), Higham & Kloeden (2005) and Alcock & Burrage (2006). For some schemes this interesting concept leads to explicit characterizations of the resulting region of mean-square stability. However, in general, stability regions need to be calculated numerically, and the choice $p = 2$ is only a special one among many that are possible and of potential interest. Important information is gained by studying the stability region as a function of p. When p increases, the cross section of the stability region of a numerical scheme shrinks as can be expected by the Lyapunov inequality. It is interesting to see for a given scheme how fast and how in detail this happens. Recall that for $\lambda < 0$ and given $p \in (0, \infty)$ the test dynamics X is p-stable when $\alpha < \frac{1}{1+\frac{p}{2}}$. We will see that it requires typically an implicit scheme to obtain, for instance, for $p = 2$ a stability region that reaches beyond $\alpha = 0.5$.

We will concentrate in this paper on the concept of p-stability for both strong and weak discrete time approximations of the test dynamics (3.5) for $\lambda < 0$ and $\alpha \in [0, 1)$. This approach provides for p close to 0 the widest stability region, which will turn out to be the one that refers to the concept of asymptotic stability as discussed in Bruti-Liberati & Platen (2008). Our aim is now to study for given strong and weak discrete time schemes the corresponding stability regions. This analysis provides valuable guidance for the choice of particular schemes and time step sizes for given numerical tasks.

We will see for many discrete time approximations Y with time step size $\Delta > 0$ when applied to the test equation (3.4) with a given degree of stochasticity $\alpha \in [0, 1)$, that the ratio

$$\left| \frac{Y_{n+1}}{Y_n} \right| = G_{n+1}(\lambda\,\Delta, \alpha) \tag{3.7}$$

is of crucial interest, $n \in \{0, 1, \ldots\}$, $Y_n > 0$, $\lambda < 0$. We call the random variable $G_{n+1}(\lambda\,\Delta, \alpha)$ the *transfer function* of the approximation Y at time t_n. It transfers the previous approximate value Y_n into the approximate value Y_{n+1} of the next time step.

Furthermore, let us assume for a given scheme and $\lambda < 0$, $\Delta \in (0, 1)$ and $\alpha \in [0, 1)$ that the random variables $G_{n+1}(\lambda\,\Delta, \alpha)$ are for $n \in \{0, 1, \ldots\}$ nonnegative, independent and identically distributed with $E((\ln(G_{n+1}(\lambda\,\Delta, \alpha)))^2) < \infty$. This assumption is satisfied for a wide range of schemes, and will allow us to obtain corresponding stability regions for all schemes that we consider by employing the following result:

Lemma 3.3 *A discrete time approximation is for given $\lambda\,\Delta < 0$, $\alpha \in [0, 1)$ and $p > 0$, p-stable if and only if*

$$E((G_{n+1}(\lambda\,\Delta, \alpha))^p) < 1. \tag{3.8}$$

The proof of Lemma 3.3 is straightforward, since it is obvious from (3.7) that the pth moment of the approximation vanishes as $n \to \infty$ if and only if $E((G_{n+1}(\lambda\,\Delta, \alpha))^p) < 1$, almost surely, for all $n \in \{0, 1, \ldots\}$.

Note that for $p > 0$, the condition (3.8) yields by the use of the inequality $\ln(x) \leq x - 1$, the relation

$$E(\ln(G_{n+1}(\lambda\,\Delta, \alpha))) \leq \frac{1}{p}\, E((G_{n+1}(\lambda\,\Delta, \alpha))^p - 1) < 0 \tag{3.9}$$

for all $n \in \{0, 1, \ldots\}$. This provides the already mentioned link to the criterion of asymptotic stability studied in Bruti-Liberati & Platen (2008) when p vanishes. A scheme is here called asymptotically stable for given $\lambda\Delta$ and α if $E(\ln(G_{n+1}(\lambda\,\Delta, \alpha))) < 0$ for all $n \in \{0, 1, \ldots\}$.

We visualize in the following the stability regions for given schemes by identifying the set of those triplets $(\lambda\,\Delta, \alpha, p)$ for which the inequality (3.8) is satisfied. We visualize in the following the stability regions for $\lambda\Delta \in [-10, 0)$, $\alpha \in [0, 1)$ and $p \in (0, 2]$. Note that when p approaches zero, we obtain the stability regions identified under the asymptotic stability criterion, see (3.9). We deliberately truncate in our visualization the stability regions at $p = 2$, since the area on the top provides information about the mean-square stability of the scheme. For higher values of p the stability region shrinks further, and for some schemes may become an empty set. Asymptotically, for very large p the stability region relates asymptotically to the worst case stability concept studied in Hofmann & Platen (1994, 1996).

4 Stability of Predictor-Corrector Methods

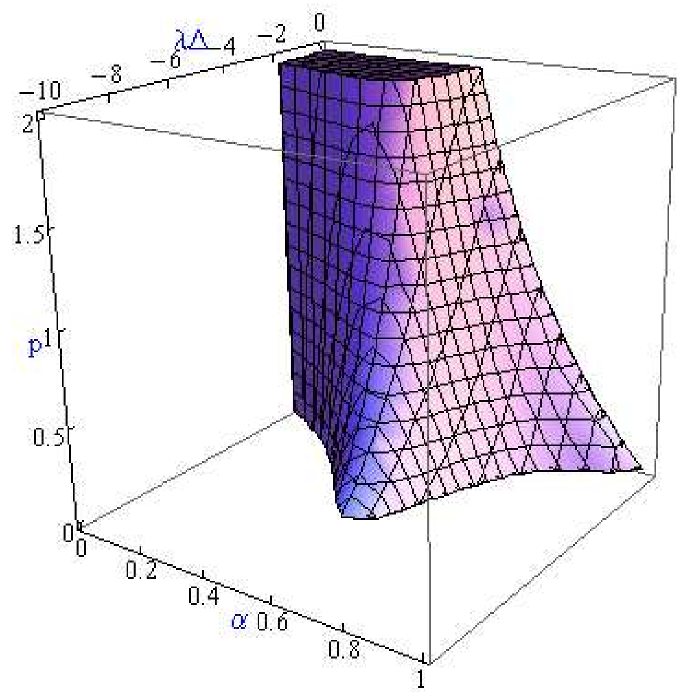

Figure 4.1: Stability region for the Euler scheme.

For the Euler scheme, which results for $\theta = \eta = 0$ in the algorithm (2.6), it follows by (3.7) that

$$G_{n+1}(\lambda\,\Delta,\alpha) = \left|1 + \left(1 - \frac{3}{2}\,\alpha\right)\lambda\,\Delta + \sqrt{-\alpha\,\lambda}\,\Delta W_n\right|, \tag{4.1}$$

where $\Delta W_n \sim \mathcal{N}(0,\Delta)$ is a Gaussian distributed random variable with mean zero and variance Δ. The transfer function (4.1) yields the stability region that is shown in Figure 4.1. It is the region where $E((G_{n+1}(\lambda\,\Delta,\alpha))^p) < 1$. This stability region has been obtained numerically by identifying for each pair $(\lambda\Delta,\alpha) \in [-10,0) \times [0,1)$ those values $p \in (0,2]$ for which the inequality (3.8) holds. One notes that for the purely deterministic dynamics of the test SDE, that is $\alpha = 0$, the stability region covers the area $(-2,0) \times (0,2)$. Also in later figures of this type we note that for $\alpha = 0$ we do not have any dependence on p. This is explained by the fact that there is no stochasticity. In this case the relation $\lambda\Delta \in (-2,0)$ reflects the classical interval of numerical stability for the Euler scheme as obtained under various criteria. For a stochasticity parameter of about $\alpha \approx 0.5$, the stability region has in Figure 4.1 the largest cross section in the direction of $\lambda\,\Delta$ for most values of p. The stability region covers an interval for $\lambda\Delta$ of increasing length up to about $[-6.5,0]$ when p is close to 0, and about $[-3,0]$ when p increases to about 2. For increased stochasticity parameter α beyond 0.5 the stability region declines in Figure 4.1. We observe that if the Euler scheme is stable for a certain step size, then it is also stable for smaller step sizes. We will see later that this is not the case for various other schemes.

The top of Figure 4.1 shows the mean-square stability region of the Euler scheme, where we have $p = 2$. As the order p of the moments increases, the cross section in the direction of α and $\lambda\Delta$ is reduced. The intuition is that as the stability requirements in terms of the order p of the moment becomes stronger, there are less pairs $(\lambda\Delta,\alpha)$ for which the simulated approximation's pth moment tends to zero.

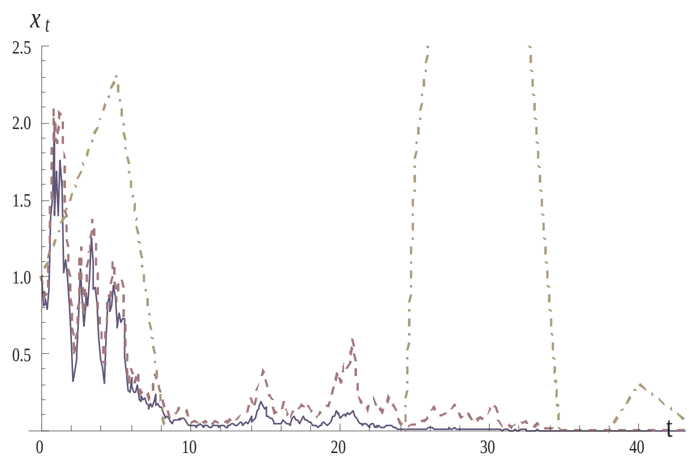

Figure 4.2: Paths of exact solution, Euler scheme with $\Delta = 0.2$ and Euler scheme with $\Delta = 5$.

To visualize the effect of numerical stability we display in Figure 4.2 a path of the exact solution and those of the corresponding Euler scheme for step sizes $\Delta = 0.2$ and $\Delta = 5$ when $\alpha = \frac{2}{3}$ and $\lambda = -1$. Note that the Euler path with the step size $\Delta = 0.2$ (dashed line) approximates the exact solution (joined line) reasonably well over the entire time period. However, the Euler path with the too large step size $\Delta = 5$ (dot-dashed line) makes no sense. The reason is that the pair $(\lambda\,\Delta, \alpha) = (-5, \frac{2}{3})$ does not belong to the stability region even for very small p.

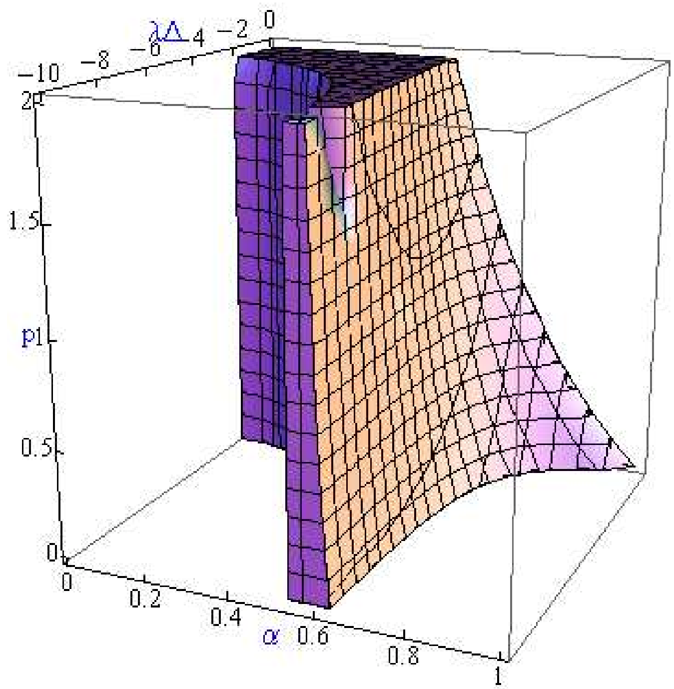

Figure 4.3: Stability region for semi-drift-implicit predictor-corrector Euler method.

Let us now consider the semi-drift-implicit predictor-corrector Euler method with $\theta = \frac{1}{2}$ and $\eta = 0$ in (2.6). The transfer function for this method equals

$$G_{n+1}(\lambda\,\Delta, \alpha) \;=\; \Bigg|1 + \lambda\,\Delta\left(1 - \frac{3}{2}\,\alpha\right)\left\{1 + \frac{1}{2}\left(\lambda\,\Delta\left(1 - \frac{3}{2}\,\alpha\right) + \sqrt{-\alpha\,\lambda}\,\Delta W_n\right)\right\} + \sqrt{-\alpha\,\lambda}\,\Delta W_n\Bigg|.$$

Its stability region is displayed in Figure 4.3. It shows that this scheme has good numerical stability around $\alpha \approx 0.6$, where it is stable nearly for all $\lambda\Delta \in [-10, 0)$. When p is close to 2, its stability region begins to show a dent around $\lambda\,\Delta \approx -9$. This means, when we consider numerical stability for the second moment $p = 2$, there could be instabilities when using step sizes leading to $\lambda\Delta \approx -9$. Unfortunately, for the stochasticity parameter value $\alpha = \frac{2}{3}$, that is when X forms a martingale, the stability region is considerably reduced compared to the one for $\alpha = 0.6$. Near the value of $\alpha = 0.6$ the semi-drift implicit predictor-corrector scheme outperforms the Euler scheme in terms of stability for most values of p.

Similarly, we obtain for the drift-implicit predictor-corrector Euler method, derived from (2.6) with $\theta = 1$ and $\eta = 0$, the transfer function

$$G_{n+1}(\lambda\,\Delta, \alpha) \;=\; \left|1 + \lambda\,\Delta\left(1 - \frac{3}{2}\,\alpha\right)\left\{1 + \lambda\,\Delta\left(1 - \frac{3}{2}\,\alpha\right) + \sqrt{-\alpha\,\lambda}\,\Delta W_n\right\}\right.$$
$$\left. + \sqrt{-\alpha\,\lambda}\,\Delta W_n\right|.$$

The corresponding stability region is plotted in Figure 4.4. It has similar features

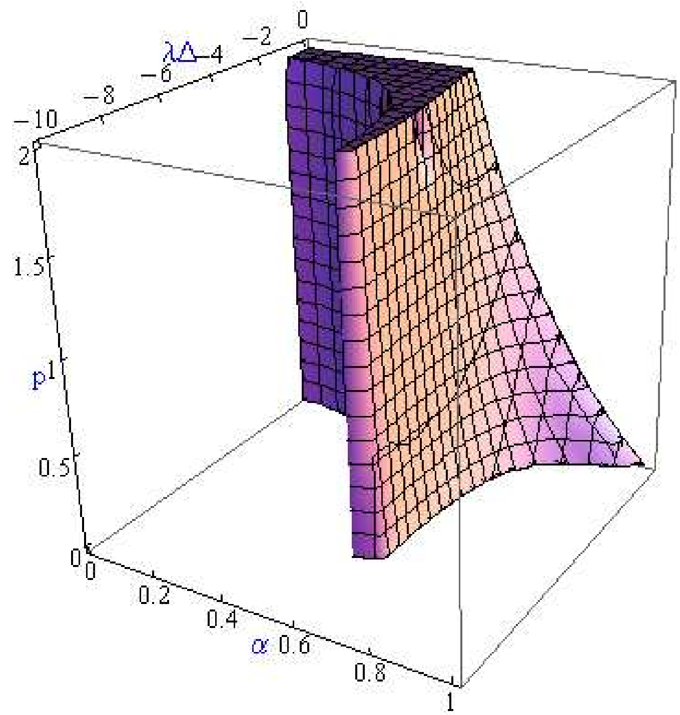

Figure 4.4: Stability region for drift-implicit predictor-corrector Euler method.

as the stability region of the semi-drift implicit predictor-corrector scheme. However, the stability region appears to be reduced. It no longer extends as far out in the direction of -$\lambda\Delta$ as in Figure 4.4. In particular, this is visible around $\alpha \approx 0.6$. When p is close to 2, the dent observed in Figure 4.3 near $\lambda\Delta \approx -9$ now occurs around $\lambda\Delta \approx -4$. It appears that the stability region has actually decreased by making the drift fully implicit. A balanced choice in (2.6) with $\theta = 1/2$ seems to be more appropriate than an extreme choice of full drift implicitness with $\theta = 1$.

Now, let us study the impact of making the diffusion term implicit in the predictor-corrector Euler method (2.6). First, we consider a predictor-corrector Euler method with semi-implicit diffusion term where $\theta = 0$ and $\eta = \frac{1}{2}$. Its transfer function has the form

$$G_{n+1}(\lambda\,\Delta,\alpha) \;=\; \Bigg|1+\lambda\,\Delta\,(1-\alpha)+\sqrt{-\alpha\,\lambda}\,\Delta W_n \\ \times\left\{1+\frac{1}{2}\left(\lambda\,\Delta\left(1-\frac{3}{2}\,\alpha\right)+\sqrt{-\alpha\,\lambda}\,\Delta W_n\right)\right\}\Bigg|.$$

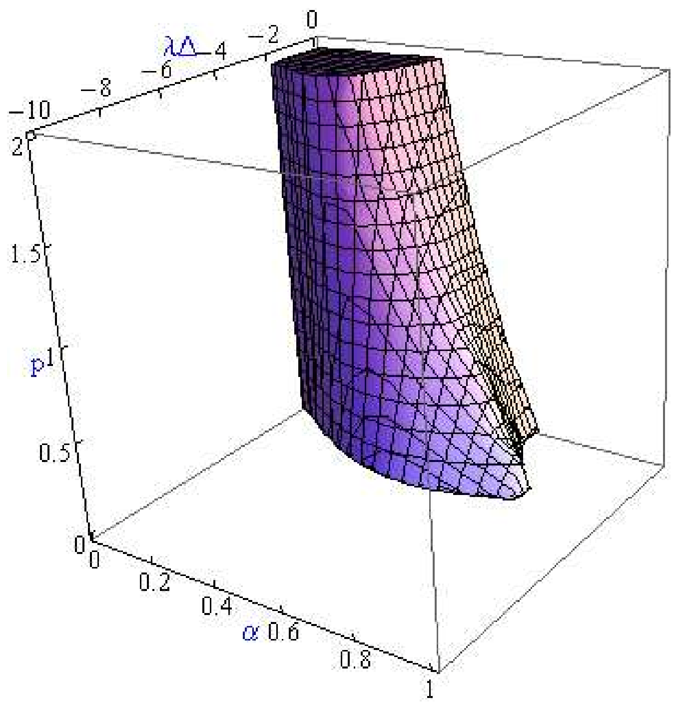

Figure 4.5: Stability region for the predictor-corrector Euler method with $\theta = 0$ and $\eta = \frac{1}{2}$.

The corresponding stability region is shown in Figure 4.5. Although it seems to be rather restricted, when compared with the one for the semi-drift implicit predictor-corrector method, it is important to note that for the martingale case, that is $\alpha = \frac{2}{3}$, the stability region is here wider than those of the previous schemes. This is an important observation, relevant for instance for applications in finance. In some sense, this could also be expected since when simulating martingale dynamics, one gains more numerical stability by making the diffusion term implicit rather than the drift term implicit which is simply zero for a martingale. Furthermore, although it may seem counter-intuitive, but for this scheme one can actually lose numerical stability by reducing the time step-size. For example, for p close to 0 and α near 0.7, we observe that for about $\lambda\Delta \approx -3$ the method is numerically stable, whereas for smaller step sizes yielding a $\lambda\Delta$ above -2, the method is no longer numerically stable. This is a phenomenon, which is not common in deterministic numerical analysis. In stochastic numerics it arises occasionally, as we will see also for some other schemes. In Figure 4.5 it gradually disappears as the value of p increases.

An interesting scheme is the symmetric predictor-corrector Euler method, obtained from (2.6) for $\theta = \eta = \frac{1}{2}$. It has transfer function

$$G_{n+1}(\lambda\,\Delta, \alpha) \;=\; \Bigg|1 + \lambda\,\Delta\,(1-\alpha)\left\{1 + \frac{1}{2}\left(\lambda\,\Delta\left(1 - \frac{3}{2}\,\alpha\right) + \sqrt{-\alpha\,\lambda}\,\Delta W_n\right)\right\}$$

$$+\sqrt{-\alpha\,\lambda}\,\Delta W_n\left\{1 + \frac{1}{2}\left(\lambda\,\Delta\left(1 - \frac{3}{2}\,\alpha\right) + \sqrt{-\alpha\,\lambda}\,\Delta W_n\right)\right\}\Bigg|.$$

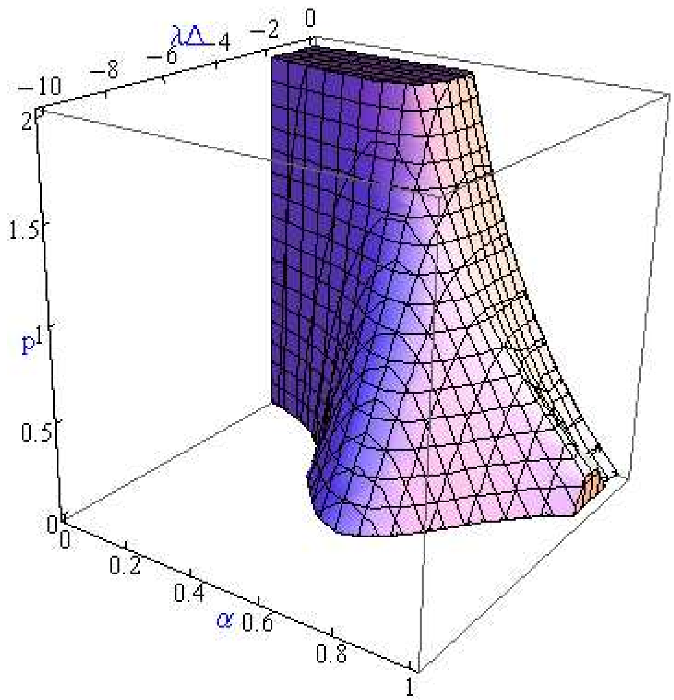

Figure 4.6: Stability region for the symmetric predictor-corrector Euler method.

Its stability region is shown in Figure 4.6. In particular, for the martingale case $\alpha = \frac{2}{3}$ it has a rather large region of stability when compared with the one of the Euler scheme and those of other previously discussed schemes. For p near zero, α close to one and $\lambda\,\Delta$ close to -1, there is a small area where this scheme is not stable. Again, this is an area where some decrease in the time step size can make a simulation numerically unstable. Also here, as the value of p increases, this phenomenon disappears.

Next we check the stability region of a fully implicit predictor-corrector Euler method, which is obtained when setting in (2.6) both degrees of implicitness to one, that is $\theta = \eta = 1$. The corresponding transfer function is then of the form

$$\begin{aligned} G_{n+1}(\lambda\,\Delta,\alpha) \;=\; & \left|1+\lambda\,\Delta\left(1-\frac{1}{2}\,\alpha\right)\left\{1+\lambda\,\Delta\left(1-\frac{3}{2}\,\alpha\right)+\sqrt{-\alpha\,\lambda}\,\Delta W_n\right\}\right. \\ & \left.+\sqrt{-\alpha\,\lambda}\,\Delta W_n\left\{1+\lambda\,\Delta\left(1-\frac{3}{2}\,\alpha\right)+\sqrt{-\alpha\,\lambda}\,\Delta W_n\right\}\right| \\ =\; & \left|1+\left\{1+\lambda\,\Delta\left(1-\frac{3}{2}\,\alpha\right)+\sqrt{-\alpha\,\lambda}\,\Delta W_n\right\}\right. \\ & \left.\times\left\{\lambda\,\Delta\left(1-\frac{1}{2}\,\alpha\right)+\sqrt{-\alpha\,\lambda}\,\Delta W_n\right\}\right|. \end{aligned}$$

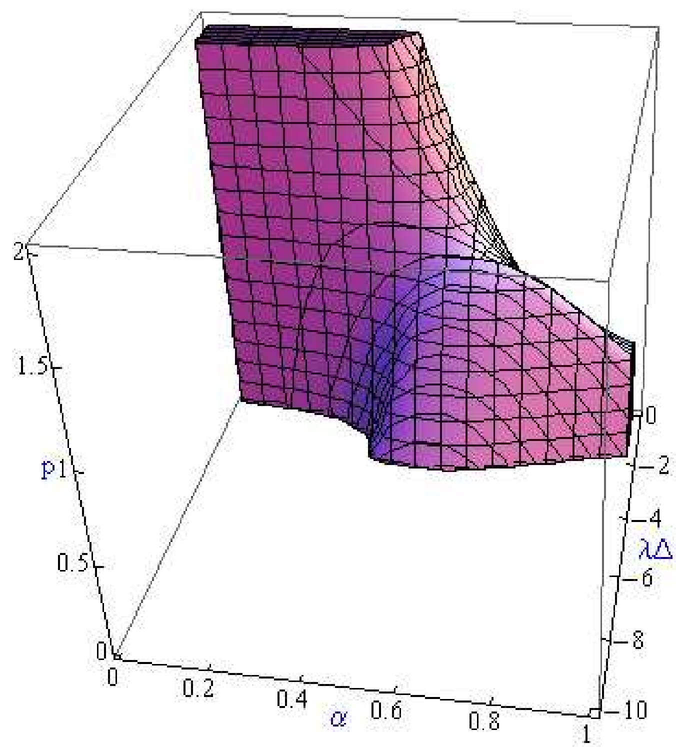

Figure 4.7: Stability region for fully implicit predictor-corrector Euler method.

The resulting stability region is shown in Figure 4.7. We notice here that this stability region is considerably smaller than that of the symmetric predictor-corrector Euler scheme. It seems that p-stability, according to our criterion, does not increase monotonically with the degree of implicitness in both the drift and the diffusion term. Balanced levels of implicitness tend to achieve the largest stability regions.

In summary, in the case of predictor-corrector Euler methods, the stability regions displayed suggest that the symmetric predictor-corrector Euler method, see Figure 4.6, is the most suitable of these for simulating martingale dynamics. The symmetry between the drift and diffusion terms of the method balances well its numerical stability properties and makes it an appropriate choice for a range of simulation tasks.

5 Stability of Some Implicit Methods

After having studied the numerical stability properties of the family of predictor-corrector Euler methods (2.6), it is worthwhile to compare the observed stability regions with those of some implicit methods, which are known to show good numerical stability properties.

Let us first consider the semi-drift implicit Euler scheme in the form

$$Y_{n+1} = Y_n + \frac{1}{2}(a(Y_{n+1}) + a(Y_n))\Delta + b(Y_n)\Delta W_n.$$

It has the transfer function

$$G_{n+1}(\lambda\,\Delta, \alpha) = \left| \frac{1 + \frac{1}{2}\,\left(1 - \frac{3}{2}\,\alpha\right)\lambda\,\Delta + \sqrt{-\alpha\,\lambda}\,\Delta W_n}{1 - \frac{1}{2}\,\left(1 - \frac{3}{2}\,\alpha\right)\lambda\,\Delta} \right|. \tag{5.1}$$

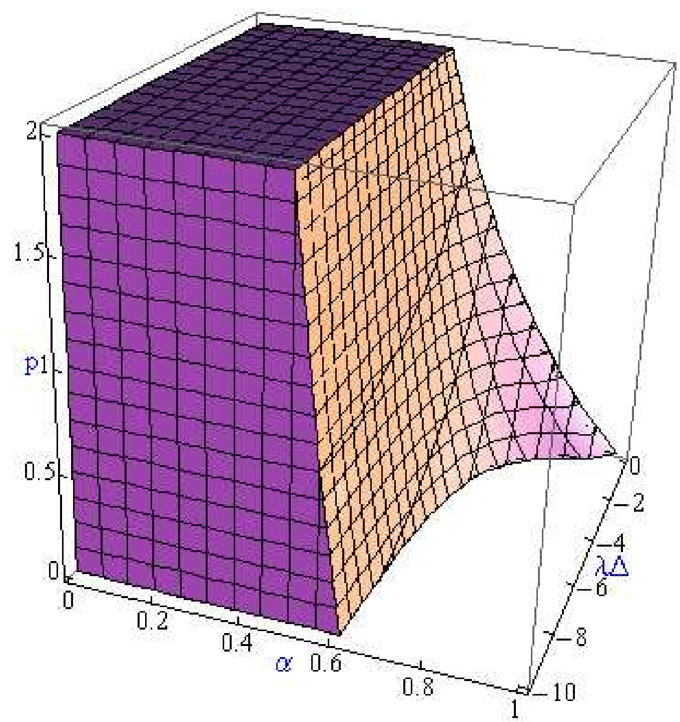

Figure 5.1: Stability region for semi-drift implicit Euler method.

Its stability region is shown in Figure 5.1. We can see from (5.1) that the transfer function involves in this case some division by α and $\lambda\Delta$. This kind of implicit scheme requires, in general, solving an algebraic equation at each time step in order to obtain the approximate solution. On the cost of this computational effort the stability region becomes significantly wider than those obtained for the previous predictor-corrector Euler schemes. For instance, for all the considered value of p and $\lambda\,\Delta$, one obtains in Figure 5.1 always numerical stability for a degree of stochasticity of up to $\alpha = 0.5$. Unfortunately, there is no stability for $\alpha = 2/3$ for any values of p when $\lambda\,\Delta < -3$, which means that this numerical scheme is not suited for simulating martingale dynamics when the step size needs to remain large. The symmetric predictor-corrector Euler method with stability region shown in Figure 4.6 appears to be still better prepared for such a task.

Now, let us also consider the full-drift implicit Euler scheme

$$Y_{n+1} = Y_n + a(Y_{n+1})\Delta + b(Y_n)\Delta W_n$$

with transfer function

$$G_{n+1}(\lambda\,\Delta, \alpha) = \left| \frac{1 + \sqrt{-\alpha\,\lambda}\,\Delta W_n}{1 - \left(1 - \frac{3}{2}\,\alpha\right)\lambda\,\Delta} \right| .$$

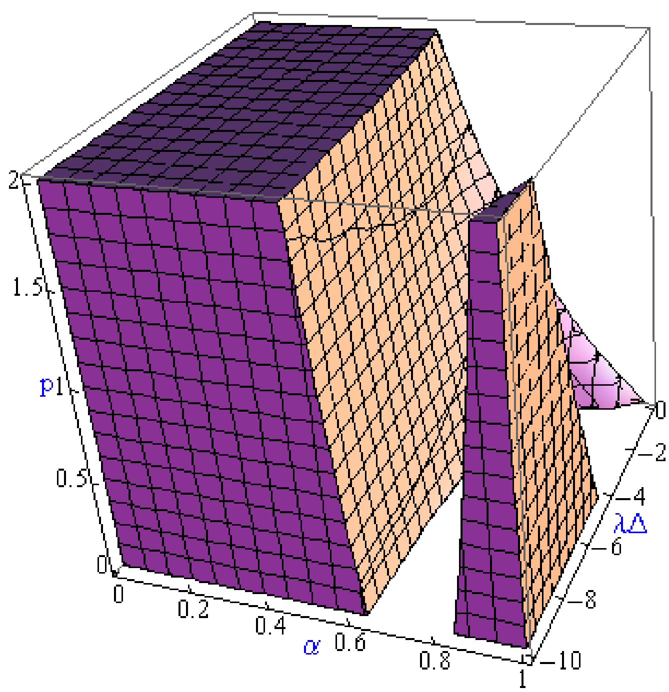

Figure 5.2: Stability region for full-drift implicit Euler method.

Figure 5.2 shows its stability region which looks similar to the region obtained for the semi-drift implicit Euler scheme. However, it has an additional area of stability for α close to 1 and $\lambda\Delta$ near -10. Also this region diminishes as p

becomes larger and does not cover the martingale case $\alpha = 2/3$. It appears that the region of stability is likely to increase with the degree of implicitness in the drift term of an implicit Euler scheme. However, this increase of stability seems to be not very strong as p becomes large.

Finally, we mention in this section the balanced implicit Euler method, proposed in Milstein, Platen & Schurz (1998). We study this scheme in the particular form

$$Y_{n+1} = Y_n + \left(1 - \frac{3}{2}\,\alpha\right) \lambda Y_n \Delta + \sqrt{\alpha|\lambda|} Y_n \Delta W_n + c|\Delta W_n|(Y_n - Y_{n+1}).$$

When c is chosen to be $\sqrt{-\alpha\,\lambda}$, then its transfer function equals

$$G_{n+1}(\lambda\,\Delta, \alpha) = \left| \frac{1 + \left(1 - \frac{3}{2}\,\alpha\right) \lambda\,\Delta + \sqrt{-\alpha\,\lambda}\,(\Delta W_n + |\Delta W_n|)}{1 + \sqrt{-\alpha\,\lambda}|\Delta W_n|} \right|.$$

The corresponding stability region is shown in Figure 5.3.

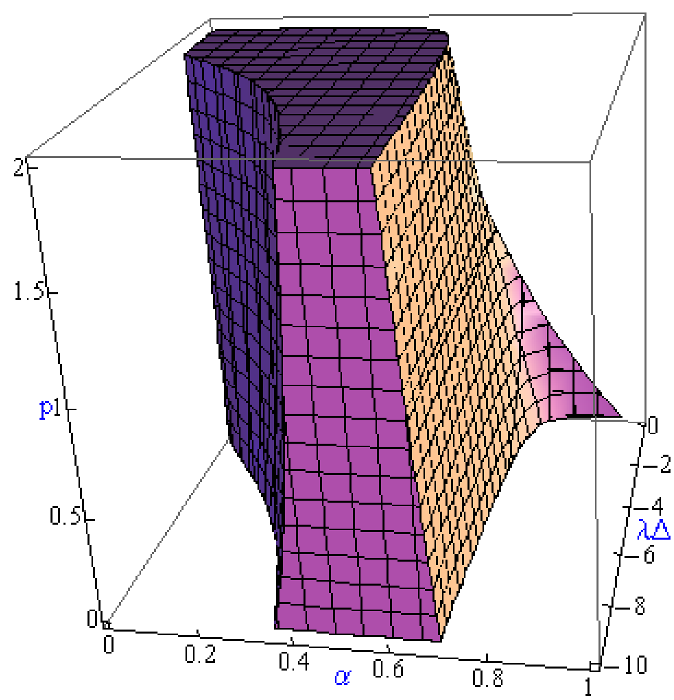

Figure 5.3: Stability region for a balanced implicit Euler method.

It turns out that this is the only type of method we considered so far that provides in the martingale case $\alpha = 2/3$ for low p numerical stability for all $\lambda\Delta$, this means, also for large step sizes. Consequently, the balanced implicit Euler method is well suited for the scenario simulation of martingales, for which it was originally designed, see Milstein, Platen & Schurz (1998). Note that one has flexibility in designing a range of balanced implicit methods, which allows to influence the stability region.

6 Stability of Monte Carlo Simulations

All the schemes we considered so far were originally designed for scenario simulation, see Kloeden & Platen (1999). However, Monte Carlo simulation requires only weak approximations. The Wiener process increments ΔW_n appearing in a Taylor scheme can be typically replaced in a weak scheme by simpler multi-point random variables, see Kloeden & Platen (1999). These need to satisfy certain moment matching conditions for a given weak order of convergence. In all previous schemes the Gaussian random variable ΔW_n may be replaced by a simpler two point distributed random variable $\Delta \hat{W}_n$, which has the following probabilities,

$$P(\Delta \hat{W}_n = \pm\sqrt{\Delta t}) = \frac{1}{2}. \tag{6.1}$$

Numerical schemes using $\Delta \hat{W}_n$ are called "*simplified*". They can be used in Monte Carlo simulation, but are not suited for scenario simulation.

We have investigated the impact of such simplification of the random variables in weak schemes on the corresponding stability regions. It turns out that the resulting stability regions look in some sense similar to those of the corresponding previously studied schemes. In most cases, the stability region increases slightly. As an example, Figure 6.1 shows the stability region of the simplified symmetric

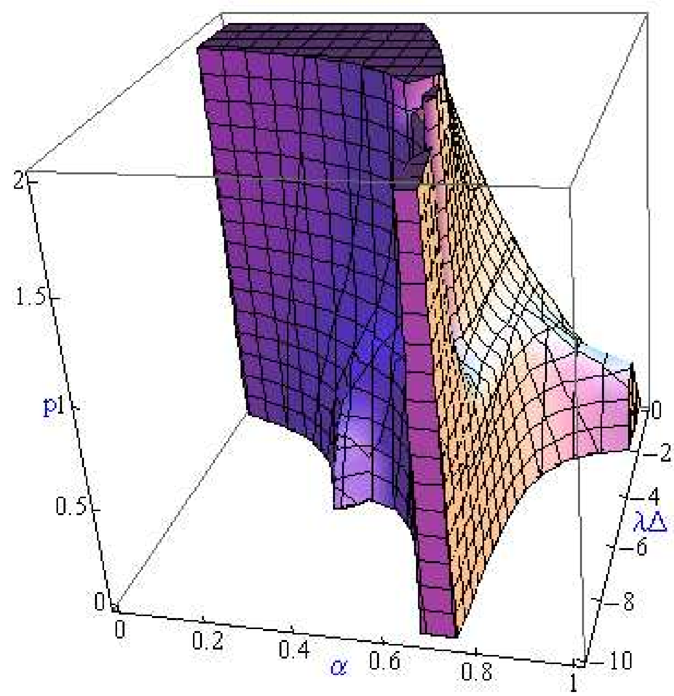

Figure 6.1: Stability region for the simplified symmetric Euler method.

predictor-corrector Euler scheme. It is, of course, different from the one displayed in Figure 4.6. When comparing these two figures, the simplified scheme shows an increased stability region, in particular, near the critical level of $\alpha = 2/3$. This is important for the Monte Carlo simulation of martingales. In general, one can say that simplified schemes usually increase numerical stability. The stability region of the simplified balanced implicit Euler method shows a very similar stability region as already given in Figure 5.3 and is, therefore, not displayed.

As pointed out in Kloeden & Platen (1999), in a simplified weak scheme also terms that approximate the diffusion coefficient can be made implicit. The reason is that one uses in a simplified scheme instead of an unbounded random variable ΔW_n a bounded random variables $\Delta \hat{W}_n$. Let us now consider the family of simplified implicit Euler schemes, see Kloeden & Platen (1999), given in the form

$$\begin{aligned} Y_{n+1} &= Y_n + \{\theta\, \bar{a}_\eta(Y_{n+1}) + (1-\theta)\bar{a}_\eta(Y_n)\}\, \Delta \\ &\quad + \{\eta\, b(Y_{n+1}) + (1-\eta)\, b(Y_n)\}\, \Delta\hat{W}_n, \end{aligned} \tag{6.2}$$

for $\theta, \eta \in [0,1]$ and $\bar{a}_\eta = a - \eta b b'$. When comparing this scheme with the strong predictor-corrector Euler scheme (2.6), one notices a resemblance to its corrector part. For sufficiently small step size Δ the implicitness in the diffusion term makes sense for this scheme. Its transfer function is of the form

$$G_{n+1}(\lambda\,\Delta, \alpha) = \frac{1 + (1 + (\eta - \frac{3}{2})\alpha)\lambda(1-\theta)\Delta + (1-\eta)\sqrt{\alpha|\lambda|}\Delta\hat{W}_n}{1 - (1 + (\eta - \frac{3}{2})\alpha)\lambda\theta\Delta - \eta\sqrt{\alpha|\lambda|}\Delta\hat{W}_n}. \tag{6.3}$$

We have studied the resulting stability regions for this family of schemes. For instance, the one for the simplified semi-drift implicit Euler scheme resembles that in Figure 5.1, and the one for the simplified full-drift implicit Euler method the one in Figure 5.2. The simplified symmetric implicit Euler scheme with $\theta = \eta = 0.5$ in (6.2) has the stability region displayed in Figure 6.2. The one for the simplified fully implicit Euler method is shown in Figure 6.3. We observe that both stability regions fill almost the entire area that we display. For this reason, a simplified symmetric or fully implicit Euler scheme could be able to overcome in a Monte Carlo simulation numerical instabilities that may arise. However, one has to be aware of the fact that with the simplified symmetric implicit Euler scheme, see Figure 6.3, there may be problems for small step sizes. For instance, for the martingale case, $\alpha = 2/3$, one may exit for $p > 0$ the stability region by decreasing the time step size. This means, for an implementation which successfully has been working for some given time step size in a derivative pricing tool, when decreasing only the time step size, one may already run into severe numerical stability problems. This type of effect has already been mentioned for several other schemes. We observe it here even for a fully implicit scheme. This suggests the following warning: Blindly refining the time step size in a Monte Carlo simulation can lead to numerical stability problems.

Finally, we perform some Monte Carlo simulations with the simplified Euler scheme and the simplified semi-drift implicit Euler scheme, where we estimate

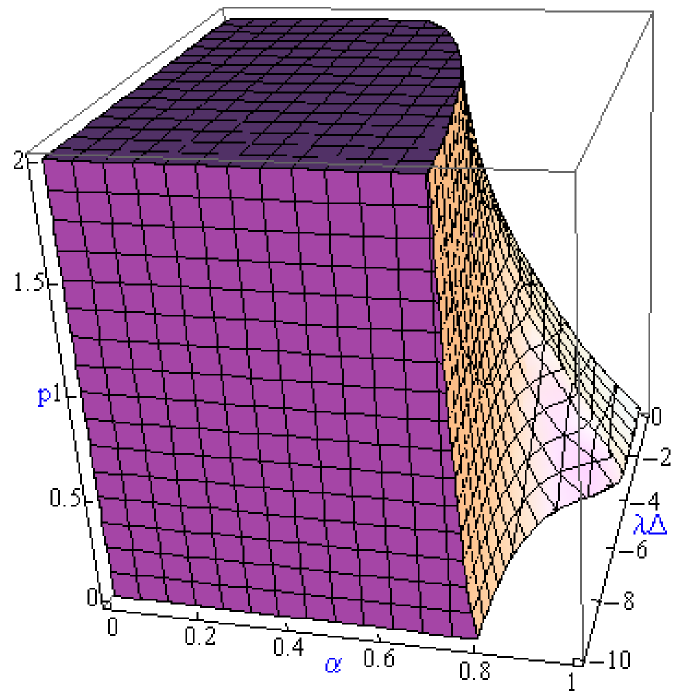

Figure 6.2: Stability region for the simplified symmetric implicit Euler Scheme.

the second moment of X_T for $T \in [3, 729]$, $\lambda = -1$, $\alpha = 0.49$ and $\Delta = 3$. We simulate $N = 1{,}000{,}000$ sample paths to obtain extremely small confidence intervals, which we subsequently neglect in Table 6.1 and show only their mid points.

T	3	9	27	81	243	729
$E(X_T^2)$	0.89	0.7	0.34	0.039	0.00006	2.17×10^{-13}
$E(\tilde{Y}_T^2)$	1.51	3.47	41.3	69796	3.47×10^{14}	9.83×10^{42}
$E(\hat{Y}_T^2)$	0.94	0.83	0.57	0.069	5.07×10^{-8}	3.0×10^{-30}

Table 6.1: Second moment of the test dynamics calculated using the exact solution X_T; the simplified Euler scheme $\tilde{Y}_T$; and simplified semi-drift implicit Euler scheme $\hat{Y}_T$.

We show in Table 6.1 the exact second moment, the one obtained via Monte Carlo simulation using the simplified Euler scheme $\tilde{Y}_T$, and the one estimated using the simplified semi-drift implicit Euler scheme $\hat{Y}_T$. One notices that the Monte Carlo simulation with the simplified Euler scheme is not satisfactory, whereas the one with the simplified semi-drift implicit Euler scheme is much better for a time horizon that is not too far out. This better performance is explained by the fact that this scheme works for $p = 2$ in its stability region, whereas the simplified Euler scheme is for the given parameter set in a region of numerical instability.

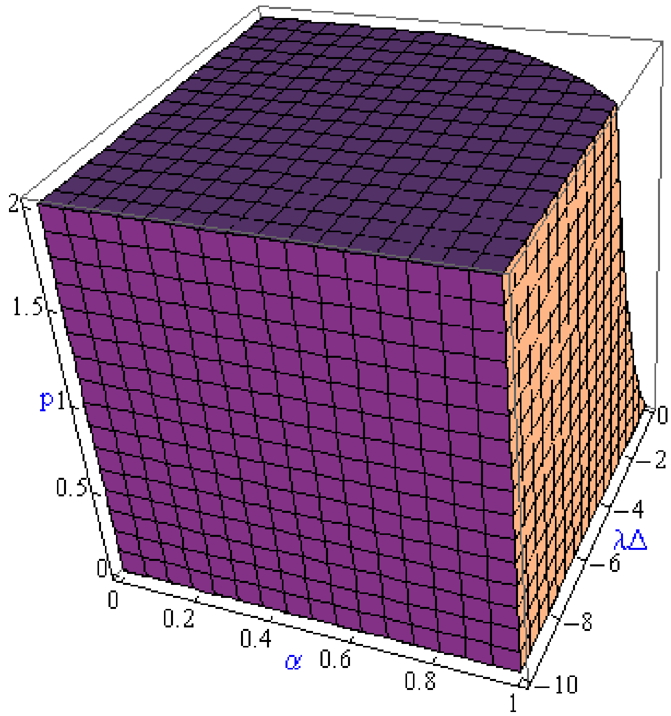

Figure 6.3: Stability region for the simplified fully implicit Euler Scheme.

Conclusion

This paper has presented a unified approach to the study of the numerical stability of discrete time approximate solutions of stochastic differential equations in finance. It has been shown that implicit methods provide the largest stability regions, whereas the standard Euler scheme has a rather restricted stability region. The symmetric predictor-corrector Euler scheme exhibits good numerical stability properties. The stability analysis of a range of schemes revealed that by refining the time step size for certain parameter ranges, the method can become numerically unstable. Simulation tools, which may have been working reliably, may fail for smaller time step sizes. The common believe that reducing the time step size always increases accuracy is not correct and may lead to serious inaccuracies.

Acknowledgment

The authors express their deep sadness about the tragic death of their dear colleague Nicola Bruti-Liberati on his way to work on 28 August 2007. He inspired some of the work presented in this paper.

References

Alcock, J. T. & K. Burrage (2006). A note on the balanced method. *BIT Numerical Mathematics* **46**, 689–710.

Bruti-Liberati, N. & E. Platen (2008). Strong predictor-corrector Euler methods for stochastic differential equations. *Stochastics and Dynamics*. (to appear).

Glasserman, P. (2004). *Monte Carlo Methods in Financial Engineering*, Volume 53 of *Appl. Math.* Springer.

Hairer, E., S. P. Nørsett, & G. Wanner (1987). *Solving ordinary differential equations I, Nonstiff problems*. Springer.

Hernandez, D. B. & R. Spigler (1992). A-stability of implicit Runge-Kutta methods for systems with additive noise. *BIT* **32**, 620–633.

Hernandez, D. B. & R. Spigler (1993). Convergence and stability of implicit Runge-Kutta methods for systems with multiplicative noise. *BIT* **33**, 654–669.

Higham, D. & P. Kloeden (2005). Numerical methods for nonlinear stochastic differential equations with jumps. *Numer. Math.* **110**(1), 101–119.

Higham, D. J. (2000). Mean-square and asymptotic stability of numerical methods for stochastic ordinary differential equations. *SIAM J. Numer. Anal.* **38**, 753–769.

Hofmann, N. & E. Platen (1994). Stability of weak numerical schemes for stochastic differential equations. *Comput. Math. Appl.* **28**(10-12), 45–57.

Hofmann, N. & E. Platen (1996). Stability of superimplicit numerical methods for stochastic differential equations. *Fields Inst. Commun.* **9**, 93–104.

Jäckel, P. (2002). *Monte Carlo Methods in Finance*. Wiley.

Klauder, J. R. & W. P. Petersen (1985). Numerical integration of multiplicative-noise stochastic differential equations. *SIAM J. Numer. Anal.* **6**, 1153–1166.

Kloeden, P. E. & E. Platen (1992). Higher order implicit strong numerical schemes for stochastic differential equations. *J. Statist. Phys.* **66**(1/2), 283–314.

Kloeden, P. E. & E. Platen (1999). *Numerical Solution of Stochastic Differential Equations*, Volume 23 of *Appl. Math.* Springer. Third printing.

Kloeden, P. E., E. Platen, & H. Schurz (2003). *Numerical Solution of SDE's Through Computer Experiments*. Universitext. Springer. Third corrected printing.

Milstein, G. N. (1988). A theorem of the order of convergence of mean square approximations of systems of stochastic differential equations. *Theory Probab. Appl.* **32**, 738–741.

Milstein, G. N. (1995). *Numerical Integration of Stochastic Differential Equations*. Mathematics and Its Applications. Kluwer.

Milstein, G. N., E. Platen, & H. Schurz (1998). Balanced implicit methods for stiff stochastic systems. *SIAM J. Numer. Anal.* **35**(3), 1010–1019.

Platen, E. (1995). On weak implicit and predictor-corrector methods. *Math. Comput. Simulation* **38**, 69–76.

Platen, E. & D. Heath (2006). *A Benchmark Approach to Quantitative Finance*. Springer Finance. Springer.

Protter, P. (2004). *Stochastic Integration and Differential Equations* (2nd ed.). Springer.

Saito, Y. & T. Mitsui (1993a). Simulation of stochastic differential equations. *Ann. Inst. Statist. Math.* **45**, 419–432.

Saito, Y. & T. Mitsui (1993b). T-stability of numerical schemes for stochastic differential equations. *World Sci. Ser. Appl. Anal.* **2**, 333–344.

Saito, Y. & T. Mitsui (1996). Stability analysis of numerical schemes for stochastic differential equations. *SIAM J. Numer. Anal.* **33**(6), 2254–2267.

Talay, D. (1982). Convergence for each trajectory of an approximation scheme of SDE. *Computes Rendus Acad. Sc. Paris, Séries I Math.* **295**(3), 249–252. (in French).